Desalination and Water Treatment
www.deswater.com
doi: 10.5004/dwt.2022.28785

270 (2022) 153–162
September

Biosorption of Cu(II) ions using sericin cross-linked with polyethylene glycol-diglycidyl ether

Geovana Silva Marques[a,*], Giovana Gonçalves Dusi[a], Fillipe Drago[a], Marcelino Luiz Gimenes[b], Vítor Renan da Silva[a]

[a]*Department of Chemical Engineering, Federal University of Paraná (UFPR), Coronel Francisco H. dos Santos Ave., 100, Curitiba, PR, 81531-980, Brazil, emails: geovana@ufpr.br (G.S. Marques), giovanadusi@gmail.com (G.G. Dusi), fillipedrago@gmail.com (F. Drago), vrenan@ufpr.br (V.R. Silva)*
[b]*Department of Chemical Engineering, State University of Maringá (UEM), Colombo Av., 5790, Maringá, PR, 87020-900, Brazil, email: marcelino@deq.uem.br*

Received 11 April 2022; Accepted 27 July 2022

ABSTRACT

In this study, a biosorbent was produced from a blend of sericin, a protein obtained from industrial waste in the silk industry, and polyethylene glycol-diglycidyl ether. For the first time, it was applied to remove Cu(II) ions from aqueous solutions. The biosorbents were characterized using scanning electron microscopy, physical adsorption of nitrogen gas, Fourier-transform infrared spectroscopy, and point-of-zero charge. A batch biosorption system determined the kinetics, equilibrium, and thermodynamic parameters. The Lagergren pseudo-first-order, pseudo-second-order, Weber–Morris diffusion, homogeneous solid diffusion, and external liquid diffusion models were used to describe the kinetics. The Langmuir, Freundlich, and Temkin models were adjusted for equilibrium modeling. The kinetic results indicated a rapid biosorption process limited to a monolayer surface. The maximum biosorption capacity was 36.17 mg g^{-1} at 20°C and a pH value of 4.77. The thermodynamic parameters indicated a spontaneous and exothermic process governed by physical interactions. The effective removal of Cu(II) ions reveals that the biosorbent is a viable alternative to conventional water treatment adsorbents and is environmentally sustainable, as it reduces the disposal of agro-industrial waste.

Keywords: Biosorption; Biosorbent; Silk sericin; Heavy metals; Spongy material; Water treatment

1. Introduction

The release of contaminated effluents is a critical environmental issue that is receiving increasing interest worldwide. Every day, large volumes of effluent contaminated with heavy metal ions are produced by industrial activities, agricultural practices, and inappropriate waste disposal [1,2]. The main characteristics of heavy metals are non-biodegradation, bioaccumulation, toxicity, and carcinogenesis [3].

Cu is a micronutrient that plays a fundamental role in the functioning of the body. However, it causes severe toxic effects at high concentrations, is considered a priority pollutant, and is a widely distributed heavy metal [4,5]. The World Health Organization establishes a maximum contaminant level of 2.0 mg L^{-1} for Cu in drinking water, and the United States Environmental Protection Agency

* Corresponding author.

1944-3994/1944-3986 © 2022 Desalination Publications. All rights reserved.

limits its concentration to 1.3 mg L^{-1} in industrial effluents. Excessive intake of Cu ions leads to kidney or liver damage and gastrointestinal issues [1,4].

Common treatments for removing heavy metal ions from polluted water include reverse osmosis, membrane filtration, distillation, ion exchange, electrochemical separation, precipitation, adsorption, and coagulation/flocculation. Among these techniques, adsorption is preferred because of its low cost, effectiveness, rapid response, and simplicity [6]. This process also enables the development of novel and inexpensive adsorbents of biological origin, such as agricultural waste [7,8], biomass [9], industrial waste [10], and polymer blends [11]. When an adsorption process utilizes biological sources as adsorbents, it is called biosorption [12].

Biosorbents derived from different materials have been used to remove Cu(II) ions from wastewater, providing suitable biosorption capacities: fruit peels [13], pequi bark [14], wood sawdust [15], almond shell [16], chitosan [17], coconut husk [18], sugarcane bagasse [19], sericin-alginate particles [20], sericin powder [21], and others.

Sericin is a hydrophilic globular protein obtained from silkworm cocoons (*Bombyx mori*) and is primarily composed of amino acids with strongly polar side groups. This represents 25%–30% of the total cocoon mass. In the silk thread industry, processing 400,000 tons of dry cocoons generates approximately 50,000 tons of sericin, which goes to waste. Typically, sericin is discarded in silk-processing wastewater during degumming, where partial hydrolysis of the silk cocoon occurs [22,23]. This disposal generates a high load of organic matter and, consequently, high biological demand, chemical oxygen demand, and nitrogen, increasing the treatment costs [24].

Sericin recovery has attracted significant attention because it exhibits beneficial properties, such as biocompatibility, biodegradability, and ultraviolet and oxidation resistance, supporting its applications for different purposes [25]. In the biosorption field, silk sericin has demonstrated potential for removing dyes, metals, and pharmaceutical contaminants. However, its broad molecular weight range (24–400 kDa), gelatinous characteristics, weak structural properties, and high water solubility form a fragile three-dimensional structure that limits the applicability of sericin biosorbents in large-scale processes [23,26].

Blending sericin with other polymers may overcome these limitations. Adsorbents from polymer blends exhibit improved characteristics compared to the components alone, such as enhanced chemical and mechanical properties, reduced costs, and superior removal efficiency [3].

Polyethylene glycol-diglycidyl ether (PEG-DE) is a synthetic polymer with amphiphilic properties. The introduction of PEG-DE into proteins occurs by cross-linking and improves stabilization and mechanical properties. In addition, it generates macroporous networks via selective dissolution, promoting the diffusion of adsorbates [3,27].

To the best of our knowledge, this is the first time a blend of sericin/PEG-DE has been employed to remove Cu(II) ions from aqueous solutions. The biosorbents produced were characterized. Batch experiments were performed to evaluate the effectiveness of the proposed method. Furthermore, the kinetics, equilibrium, and thermodynamics of biosorption were investigated.

2. Materials and methods

2.1. Materials

Silkworm cocoons (*Bombyx mori*) were provided by producers in the northwest region of Paraná (Brazil). Polyethylene glycol-diglycidyl ether (PEG-DE, average M_n 500) was supplied by Sigma-Aldrich (United Kingdom).

Batch biosorption experiments were performed by diluting $CuSO_4 \cdot 5H_2O$ (Vetec) with distilled water. Complexation with cuprizone (oxalic acid bis[cyclohexylidene hydrazide], 98%, Across), anhydrous ethanol (99.5%, Sigma-Aldrich), and phosphate buffer prepared with $K_2HPO_4 \cdot 3H_2O$ (98%, Vetec) and KH_2PO_4 (98%, Vetec) was applied to quantify Cu(II) ions.

2.2. Sericin extraction

Sericin extraction via degumming was conducted as described by Silva et al. [28]. Silkworm cocoons (7.5 g) were cut into 1.0 cm^2 pieces and placed in 250 mL distilled water in Erlenmeyer flasks. Degumming was performed in an autoclave (Phoenix, Brazil, Model AV – 30) at 120°C for over 20 min. The suspension was then vacuum-filtered while hot. Because the obtained sericin solution was diluted, it was heated in a bath (Quimis, Brazil, Model G215M1) until its concentration reached 3% w/w.

2.3. Biosorbent preparation

Three formulations were prepared following the technique described by Tao et al. [25], with modifications to produce a material with suitable structural characteristics as a biosorbent. Different PEG-DE proportions were added to the sericin solution under heat and constant mechanical stirring (Fisatom, 715 W), depending on the mass of the sericin (1:0.5, 1:1, and 1:2). The mixed solutions were poured into stainless steel dishes and frozen at −20°C. Next, they were dried via sublimation in a freeze-dryer (Liotop L101, Liobras) at −50°C for 24 h. Spongy materials were obtained and cut into pellets of approximately 8 mm^3.

2.4. Biosorbent characterization

The biosorbent with the most suitable mechanical properties, particularly stiffness and fragility, was characterized using scanning electron microscopy (SEM), nitrogen adsorption–desorption isotherms, Fourier-transform infrared spectroscopy (FTIR), and the point-of-zero charge (pH_{PZC}).

Surface and cross-sectional morphologies were examined using a scanning electron microscope (JSM-6360LV, JEOL, Japan). The biosorbent samples were placed on aluminum stubs using double-sided adhesive tape and coated with a thin layer of Au. SEM images were captured at an acceleration potential of 15 kV and amplification of 50×.

Nitrogen adsorption–desorption isotherms were obtained at 77 K and pressures ranging from 1.2×10^{-3} to 0.092 MPa (Micromeritics ASAP 2020). The specific area was determined using the Brunauer–Emmett–Teller (BET) equation [29], and the pore volume was calculated using single-point adsorption based on $P/P_0 = 1$.

Information about functional groups and chemical properties was obtained using a transformed infrared

spectrophotometer (Vertex 70v, Bruker, Germany) and the KBr pellet method (P.A., Vetec, Brazil) with compression of eight tons. All analyses were performed with a 4 cm^{-1} scan resolution recorded between 4,000–400 cm^{-1}.

Additionally, the pH_{PZC} value of the biosorbent was determined as described by Hameed et al. [30], with modifications. This experiment was performed by adding 30 mg biosorbent to a 30 mL KCl (P.A., Vetec, Brazil) solution (0.1 mol L^{-1}) under 11 initial pH conditions (2, 3, 4, 5, 6, 7, 8, 9, 10, 11, 12) adjusted with 0.1 mol L^{-1} HCl (P.A., ISOFAR, Brazil) or 0.1 mol L^{-1} NaOH (P.A., Êxodo Científica, Brazil). The solutions were maintained under agitation in a temperature-controlled orbital shaker (TE-421, Tecnal, Brazil) at 25°C for 24 h. The final pH of each solution was then measured. A graph of the initial pH vs. final pH was plotted, and pH_{PZC} was defined as the range where the final pH remained constant, despite the initial pH.

2.5. Batch biosorption

Batch biosorption experiments were conducted by adding 60 mg of the biosorbent to 60 mL Cu(II) ion solution in Erlenmeyer flasks. The flasks were subjected to constant agitation (150 rpm) in an incubator shaker (TE-421, Tecnal, Brazil) at different temperatures at a specific time. The samples were then filtered, and Cu(II) concentrations were determined using an ultraviolet-visible spectrophotometer (UV 1800, Shimadzu) through the complexation of the Cu(II) with hydroalcoholic solution (50% v/v) of cuprizone in slightly alkaline medium (phosphate buffer, pH 8–9.5) [31]. Absorbance was measured at a wavelength of 600 nm using 10 mm quartz cuvettes [32]. A calibration curve of Cu(II) concentration vs. absorbance was obtained with a correlation coefficient of 0.99.

The biosorption uptake q (mg g^{-1}) was calculated using Eq. (1):

$$q = \frac{\left(C_0 - C\right)\cdot V}{w} \tag{1}$$

where C_0 (mg L^{-1}) is the initial concentration of Cu(II) ions, C (mg L^{-1}) is the liquid-phase concentration of Cu(II) ions at time t (min), V (mL) is the volume of the solution, and w (g) is the mass of the biosorbent.

The effect of the pH solution on the amount of adsorbed Cu(II) ions was evaluated by varying the pH solution (2, 3, 4, 4.77, and 5) at a fixed initial concentration of Cu(II) (25 mg L^{-1}), temperature (20°C), and time (2 h). The pH was adjusted using aqueous solutions of HCl or NaOH (0.1 mol L^{-1}).

A kinetic study was conducted to evaluate the effect of the contact time on biosorption and the mechanism controlling the process. Tests were performed at 20°C, 40°C, and 60°C and an initial concentration of 25 mg L^{-1} Cu(II) solution. Samples were collected at 2, 5, 10, 30, 60, 120, and 180 min.

In addition, equilibrium isotherms were obtained at 20°C, 40°C, and 60°C by varying the initial concentration of the Cu(II) solution (25, 40, 60, 80, and 100 mg L^{-1}). The flasks were agitated for 72 h.

2.6. Biosorption kinetic models

Biosorption data can be described using several mathematical models, classified as adsorption reaction and adsorption diffusion [33]. The following models were applied for kinetic data fitting to clarify the mechanisms and evaluate Cu(II) biosorption: Lagergren pseudo-first-order, pseudo-second-order, Weber–Morris intraparticle diffusion, homogeneous solid diffusion model (HSDM), and external liquid-film diffusion.

The Lagergren pseudo-first-order model describes the physical adsorption between the adsorbate and adsorbent, representing their reversible interactions. This model is expressed by Eq. (2):

$$\frac{dq}{dt} = K_1 \cdot \left(q_{EQ} - q\right) \tag{2}$$

where $q(t)$ and q_{EQ} (mg g^{-1}) are the amounts of Cu(II) adsorbed at time t (min) and equilibrium, respectively, and K_1 (min^{-1}) is the kinetic constant for the pseudo-first-order model.

The pseudo-second-order model describes strong interaction forces between the adsorbate and adsorbent during adsorption, as by chemical linkages. It is expressed by Eq. (3):

$$\frac{dq}{dt} = K_2 \cdot \left(q_{EQ} - q\right)^2 \tag{3}$$

where K_2 (g mg^{-1} min^{-1}) is the kinetic constant for the pseudo-second-order model.

The Weber–Morris intraparticle diffusion model can be applied to identify successive mass transfer steps and predict the limiting step of the process [9]. This model is expressed by Eq. (4):

$$q\left(t\right) = K_{WM} \cdot \sqrt{t} \tag{4}$$

where K_{WM} is the Weber–Morris intraparticle diffusion model constant (mg g^{-1} $min^{-1/2}$).

HSDM provides the exact solution to the differential mass balance in an amorphous and homogeneous sphere, considering the diffusive effect of the solute and neglecting the external film resistance [33]. The HSDM solution, in terms of the average adsorption quantity of the solute in the solid ($\bar{q}$), is written as follows:

$$\bar{q}\left(t\right) = q_{EQ} \cdot \left\{1 - \frac{6}{\pi^2}\sum_{n=1}^{\infty}\frac{1}{n^2}\exp\left(-n^2.K_D.t\right)\right\} \tag{5}$$

where K_D is the diffusion constant.

2.7. Biosorption equilibrium

Equilibrium data provide information about the maximum biosorption capacity of the biosorbent, which is critical for assessing its performance. They can be described by adsorption isotherms, in which the parameters express the biosorbent surface properties and affinity between the adsorbent and adsorbate [22].

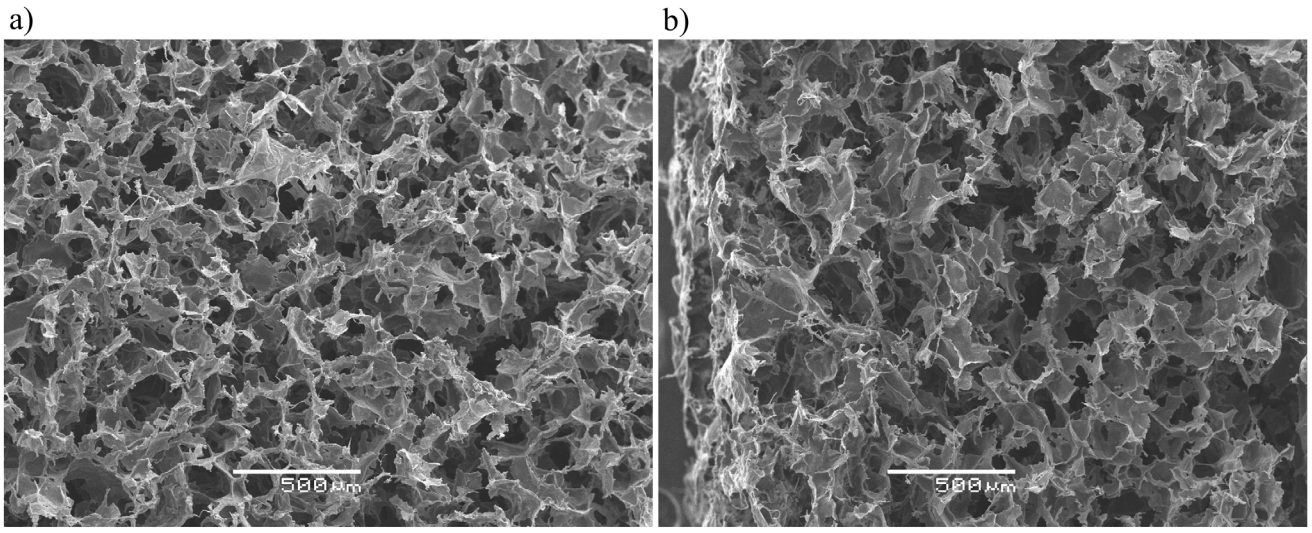

Fig. 1. Morphology of sericin/PEG-DE material: (a) surface and (b) cross-section.

The Langmuir isotherm assumes adsorption as a monolayer process on a homogeneous surface with a finite number of identical sites [9]. This model is expressed by Eq. (6):

$$q_{EQ} = \frac{q_M \cdot K_L \cdot C_{EQ}}{1 + K_L \cdot C_{EQ}} \tag{6}$$

where q_{EQ} (mg g^{-1}) is the amount adsorbed at equilibrium, q_M is the maximum adsorption capacity, C_{EQ} is the equilibrium concentration of the Cu(II) solution (mg L^{-1}), and K_L is the Langmuir equilibrium constant (L mg^{-1}).

The empirical Freundlich isotherm model is based on heterogeneous surfaces or surfaces with different affinities. This model suggests that the stronger binding sites are occupied first, and as the number of occupied sites increases, the binding strength decreases [30]. The model is expressed by Eq. (7):

$$q_{EQ} = K_F \cdot C_{EQ}^{\frac{1}{n}} \tag{7}$$

where K_F is the Freundlich constant (mg g^{-1}[L/mg]$^{1/n}$) related to the adsorption capacity, and n is the heterogeneity factor related to the adsorption intensity.

The Temkin isotherm [Eq. (8)] considers the adsorbent–adsorbate interactions, and the heat of adsorption of all molecules in the layer decreases linearly with coverage. The Temkin isotherm assumes a uniform distribution of binding energies up to the maximum binding energy [30]:

$$q_{EQ} = \frac{R.T}{b} \cdot \ln\left(K_T \cdot C_{EQ}\right) \tag{8}$$

where R is the ideal gas constant (8.314 J mol^{-1} K^{-1}), T is the adsorption temperature, b is the heat of adsorption (J g mg^{-2}), and K_T (L mg^{-1}) is the Temkin constant.

Data fitting was performed via nonlinear regression analysis, and the suitability of the kinetic and isotherm models was based on the coefficient of determination (R^2) and mean relative percentage error (MRE) at a 95% confidence level. Statistica software (version 12, USA) was used for all data analyses.

2.8. Estimation of thermodynamic parameters

Thermodynamic analysis was conducted to predict the Cu(II) biosorption nature. The parameters were estimated from the equilibrium constant (K_{EQ}) at each temperature. K_{EQ} values were calculated from a graph, $\ln(q_{EQ}/C_{EQ})$ vs. C_{EQ}, extrapolating C_{EQ} to zero [34].

After K_{EQ} was known, the standard Gibbs free energy of biosorption (ΔG) was calculated using Eq. (9):

$$\Delta G = -R \cdot T \cdot \ln K_{EQ} \tag{9}$$

where R is the universal constant of gases (8.314 J mol^{-1} K^{-1}), and T is the temperature (K).

The enthalpy (ΔH) and entropy (ΔS) of biosorption were determined using Eq. (10) by plotting $\ln(K_{EQ})$ vs. $1/T$. The slope of the equation corresponds to $\Delta H/R$, and the linear coefficient corresponds to $\Delta S/R$.

$$\ln K_{EQ} = \frac{\Delta S}{R} - \frac{\Delta H}{R \cdot T} \tag{10}$$

3. Results and discussion

3.1. Biosorbent characterization

The 1:0.5 ratio (mass of sericin to the mass of added PEG-DE) resulted in brittle materials, whereas the 1:2 ratio formed materials with a rubbery appearance. The 1:1 ratio yielded less brittle biosorbents with suitable stiffness; then, these biosorbents were characterized.

Surface and cross-sectional micrographs of the biosorbent (Fig. 1) show a porous structure with a heterogeneous pore distribution and irregular morphology, as observed

by Tao et al. [25]. Pores are formed after ice sublimation during the freeze-drying process, and their sizes are determined by the size of the ice crystals formed during freezing. A higher freezing temperature favors larger pore formation [25,35].

Nitrogen adsorption–desorption isotherms indicated a BET surface area of 1.86 $m^2\ g^{-1}$, pore volume of 8.7 × $10^{-4}\ cm^3\ g^{-1}$, and average pore width of 1.87 nm. The surface area value is close to that obtained for commercial powdered sericin (1.5 $m^2\ g^{-1}$) [36]. This similarity suggests that chemical cross-linking with PEG-DE did not damage the sericin surface area, enabling the application of the sericin/PEG-DE material as a biosorbent.

Fig. 2 shows the FTIR spectra of the biosorbent. The spectra presented characteristic amide absorption bands of protein. The absorption peak at approximately 1,652 cm^{-1} represents the C=O stretching vibration of the amide group and is attributed to amide I; the absorption peak at approximately 1,519 cm^{-1} refers to amide II and represents N–H bending and C–N stretching vibration; the peak at approximately 1,247 cm^{-1} was associated with amide III from the C–N stretching vibration to the N–H in-plane bending vibration [37]. The absorption peak at approximately 3,300 cm^{-1} represents the stretching vibration of the O–H groups in a polymeric association. The 3,000–2,800 cm^{-1} range was assigned to $–CH_2–$ stretching [23]. Moreover, the peak at approximately 1,114 cm^{-1} was assigned to the stretching of the C–O–C bond of PEG-DE, confirming that the PEG-DE chains were introduced into the sericin. In cross-linking, aliphatic and aromatic hydroxyl groups of serine and tyrosine residues of sericin are the reaction sites [27].

Considering the functional groups identified in the FTIR spectra and that Cu(II) ions preferentially bind to oxygen [2], the –C=O and –OH groups are likely to participate in Cu bonding. These bonds were abundant in sericin and PEG-DE.

3.2. Biosorption studies

pH_{PZC} was determined to reveal the biosorbent surface charge under the experimental conditions. From the constant zone of the initial pH vs. final pH graph (Fig. 3), the pH_{PZC} value was found to be 5.68. Above this value, the biosorbent surface is negatively charged, whereas, below this value, it is positively charged [1]. Because Cu exists in its predominantly cationic form (Cu^{2+}), a negatively charged surface favors Cu uptake.

The acidity of the solution is also a fundamental factor in metal ion biosorption because it results in protonation or deprotonation of the functional groups of the biosorbent. The biosorption of the Cu(II) ions onto the developed biosorbent over a range of the pH values of the solution was investigated (Fig. 4).

The pH of the solution significantly influenced Cu(II) removal, and the highest removal capacities occurred at pH = 4.77 (13.40 mg g^{-1}) and pH = 5 (13.52 mg g^{-1}). At lower pH values, the removal capacity decreases once fewer functional groups are ionized, and a high concentration of H^+ leads to competition with Cu(II) for the active sites. Conversely, higher pH values increase the number of negatively charged sites and the electrostatic attraction between the surface and ions, facilitating biosorption [3,36].

It is important to note that for pH > 6, Cu(II) ions precipitate as $Cu(OH)_2$ [10], and the results for pH = 4.77 and pH = 5 were statistically equal. Thus, the pH value was

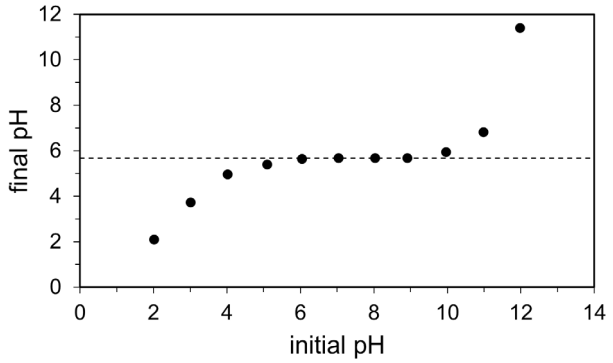

Fig. 3. Determination of pH_{PZC}.

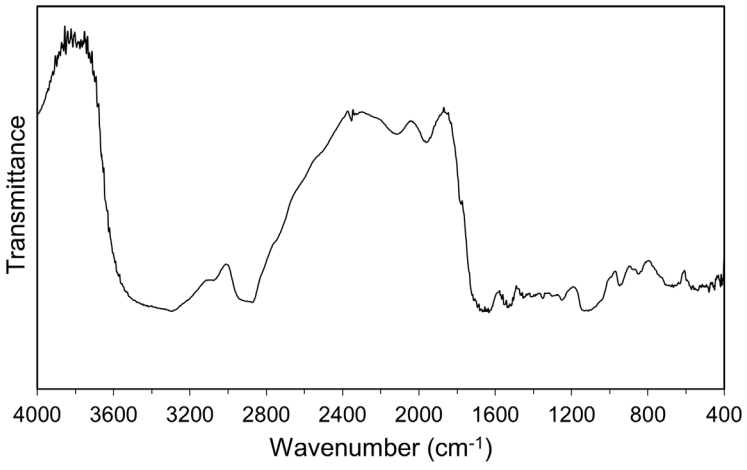

Fig. 2. FTIR spectra of sericin/PEG-DE material.

fixed at 4.77 (obtained directly by dissolving $CuSO_4 \cdot 5H_2O$ in distilled water) to conduct kinetic and equilibrium studies.

3.3. Biosorption kinetics

Biosorption kinetics provide essential information regarding the biosorption mechanism, which is related to the rate-limiting steps of the process and crucial for metal removal studies [3,38]. Fig. 5 shows the biosorption capacity as a function of time at a pH value of 4.77 and an initial Cu(II) concentration of 25 mg L^{-1}. At all applied temperatures (20°C, 40°C, and 60°C), Cu(II) biosorption occurred rapidly, and most ions were adsorbed within 10 min of contact between the biosorbent and solution. As the available sites were filled, the biosorption rate decreased until the material reached saturation. After 180 min, the Cu(II) removal value ranged between 61.3% and 66.8%.

The kinetic data were adjusted to different models. The kinetic parameters are listed in Table 1. Coefficients of determination (R^2) exceeding 98.45% and minor mean errors (0.17%–0.47%) indicate that the pseudo-second-order model best fits the experimental data. In this model, the variation in the adsorbed mass over time was delimited by the quadratic concentration gradient, leading to an improved fit of the initial transient biosorption. It is also assumed that the rate-limiting step in the biosorption process may be chemical sorption involving valence forces by sharing or exchanging electrons between active sites and metal ions [3]. As the interaction between the negatively charged functional groups of the biosorbent and the cationic ion Cu^{2+} is specific, the process is rapid and limited by the availability of active sites (–C=O, –OH) in the biosorbent. Thus, the adsorption reaction models described the biosorption process.

The intraparticle diffusion Weber–Morris model presented a poor fit to the experimental data, with the lowest R^2 values (26.91%–31.02%) and the highest mean relative error (49.1%). This suggests that internal mass transfer is not an important resistance mechanism. As the Van der Waals radius of Cu is 0.14 nm [1], significantly smaller than the average pore width of the biosorbent (1.86 nm), Cu(II) ions may not have access resistance to biosorption.

Although the HSDM approached the Lagergren pseudo-first-order and pseudo-second-order models, it was not predictive because it did not describe the initial transient biosorption, only an equilibrium region. The resistance related to the Cu(II) ion diffusion from the solution to the biosorbent interface might be reduced by the favorable conditions of the balanced charge applied.

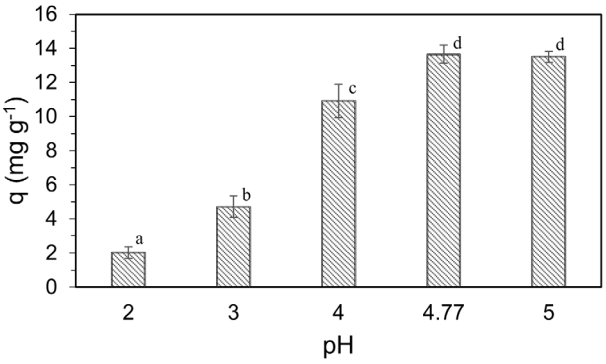

Fig. 4. Effect of pH of the solution on Cu(II) biosorption. *Means with the same letters represent no statistical differences according to Tukey's test ($p < 0.05$).

3.4. Biosorption equilibrium

Experimental isotherms express the relationship between the adsorbate equilibrium concentration in the solution (C_{EQ}) and solid phase (q_{EQ}) at an established temperature, which helps clarify the performance of the biosorption system [39]. Thus, the Langmuir, Freundlich, and

Table 1
Kinetic parameters of Cu(II) biosorption onto sericin/PEG-DE biosorbent

Kinetic models	Parameters	20°C	40°C	60°C
Lagergren pseudo-first-order model	K_1 (min^{-1})	1.13 ± 0.09	1.03 ± 0.04	1.27 ± 0.08
	q_{max} (mg g^{-1})	16.44 ± 0.12	16.07 ± 0.15	15.16 ± 0.07
	R^2	85.08	83.89	88.10
	MRE (%)	1.38	1.77	0.88
Pseudo-second-order model	K_2 (g mg^{-1} min^{-1})	0.234 ± 0.005	0.19 ± 0.01	0.35 ± 0.01
	q_{max} (mg g^{-1})	16.68 ± 0.02	16.35 ± 0.05	15.32 ± 0.02
	R^2	99.70	98.45	99.38
	MRE (%)	0.17	0.47	0.25
Intraparticle diffusion Weber–Morris	K_{WM} (mg g^{-1} $min^{-0.5}$)	1.80 ± 0.46	1.76 ± 0.44	1.66 ± 0.43
	R^2	28.83	31.02	26.91
	MRE (%)	48.9	48.4	49.1
Homogeneous solid diffusion model (HSDM)	K_C	0.80 ± 0.08	0.66 ± 0.08	0.95 ± 0.08
	q_{max} (mg g^{-1})	16.71	16.51	15.32
	R^2	92.34	80.76	89.03
	MRE (%)	1.46	2.40	0.96

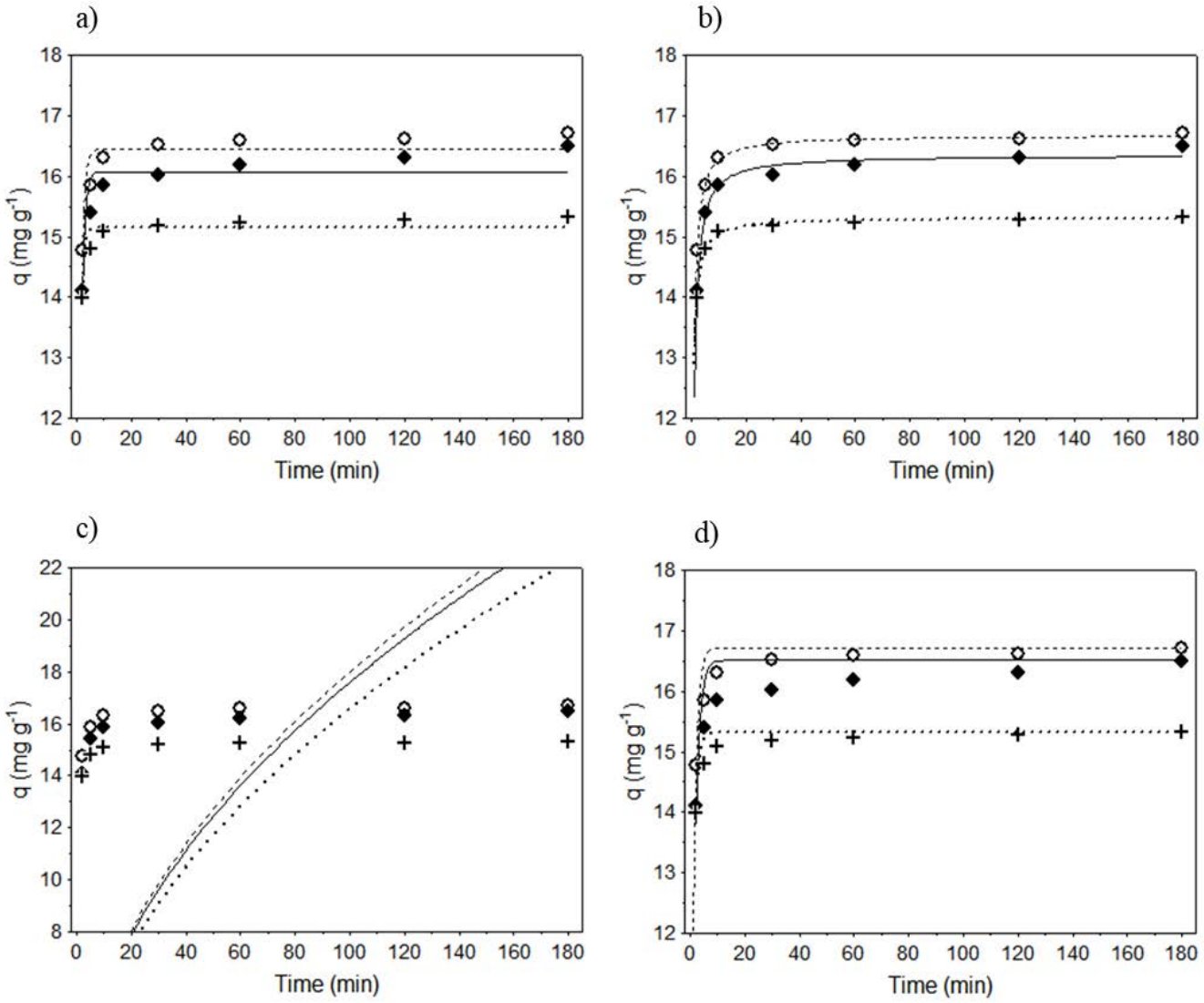

Fig. 5. Kinetics of Cu(II) ions biosorption onto sericin/PEG-DE. (a) Lagergren pseudo-first-order model, (b) pseudo-second-order model, (c) intraparticle diffusion Weber–Morris model, and (d) Homogeneous solid diffusion model. Experimental data: ○ 20°C; ♦ 40°C; + 60°C. Modeling data: --- 20°C; — 40°C; ····· 60°C.

Temkin models were adjusted to equilibrium data at 20°C, 30°C, and 40°C. Fig. 6 shows the curves, and Table 2 lists the isotherm parameters.

The Langmuir isotherm showed the best fit to the experimental data for all temperatures, with R^2 ranging from 99.01% to 99.53% and the smallest mean errors (0.66%–2.99%). This suggests that monolayer adsorption was the primary biosorption mechanism for Cu(II) removal and the sericin/PEG-DE surface had binding sites of equal affinity and energy. Therefore, it could reach saturation [3]. The maximum biosorption capacity was 36.17 ± 1.81 mg g^{-1} at 20°C. As the temperature increased, the maximum biosorption capacity decreased, indicating an exothermic process. Similar maximum biosorption capacity values have been reported for Cu(II) ions biosorption onto various biosorbents, such as black tea waste (43.2 mg g^{-1}) [40], peanut shells (25.4 mg g^{-1}) [41], rice straw (18.4 mg g^{-1}) [8], and chitosan/glutaraldehyde beads (31.20 mg g^{-1}) [42].

Although the Freundlich and Temkin isotherms indicated an acceptable fit to the multilayer biosorption process, these models showed lower variable R^2 values (90.50%–99.20%) and mean errors ranged from 1.62% to 14.09%, suggesting a higher modeling predictive deviation than the Langmuir isotherm model. The adsorbed mass curves in equilibrium revealed that the biosorption capacity of the biosorbent was limited to the surface, regardless of the concentration in the solution.

These results indicate that Cu(II) biosorption onto the porous biosorbent is a surface phenomenon that occurs through electrostatic interactions between the Cu(II) ions and the negatively charged functional groups of the biosorbent at pH = 4.77. Thus, biosorption occurs while functional groups are available. When the sites are tightly bound, equilibrium

Table 2
Isotherm parameters for Cu(II) ions biosorption onto sericin/PEG-DE

Isotherm models	Parameters	20°C	40°C	60°C
Langmuir	q_{max} (mg g^{-1})	36.17 ± 1.81	24.36 ± 0.84	18.76 ± 0.18
	K_L (L mg^{-1})	0.049 ± 0.002	0.23 ± 0.05	0.150 ± 0.007
	MRE (%)	0.67	2.99	0.66
	R^2	99.01	99.30	99.53
Freundlich	K_F (mg g^{-1}(L/mg)$^{1/n}$)	4.39 ± 0.64	8.07 ± 1.10	5.35 ± 1.26
	N	2.29 ± 0.20	3.81 ± 0.73	3.48 ± 0.81
	MRE (%)	2.90	7.52	6.09
	R^2	98.04	90.50	94.13
Temkin	K_T (L mg^{-1})	6.91 ± 1.01	10.23 ± 1.44	10.13 ± 1.08
	B	618.90 ± 94.4	73,269 ± 43.52	1,057.29 ± 21.04
	MRE (%)	14.09	3.64	1.62
	R^2	91.48	98.60	99.20

Table 3
Thermodynamic data for Cu(II) ions biosorption onto sericin/PEG-DE

Temperature (K)	K_{EQ}	ΔG (kJ mol^{-1})	ΔH (kJ mol^{-1})	ΔS (kJ K^{-1} mol^{-1})
293.15	1.17	–0.385		
313.15	2.67	–2.555	–20.1	+0.071
333.15	3.11	–3.146		

between the solution concentration and the retained Cu(II) mass is reached.

3.5. Thermodynamic study

The effect of the temperature (at 20°C, 40°C, and 60°C) on Cu(II) biosorption onto the biosorbent was evaluated. The thermodynamic parameters are listed in Table 3.

The ΔG values were negative at all temperatures, so biosorption was spontaneous at the investigated pH values. In addition, the decrease in the Gibbs free energy with increasing temperature reveals that the process becomes more spontaneous, indicating that the increased temperature favors biosorption. The same trend was observed for Cu(II) biosorption onto hazelnut shells, which was attributed to an increase in pore size and kinetic energy of the ions as the temperature increased, facilitating contact with the biosorbent [41].

The ΔH value of −20.1 kJ mol^{-1} reveals an exothermic biosorption process, and the interactions between the Cu(II) ions and biosorbent were predominantly physical [43]. The positive value of ΔS suggests increased randomness at the solid-solution interface, attributed to adsorbate species that gain translational entropy by displacing biod water molecules, which maintains randomness in the system [3].

4. Conclusions

This study demonstrates that the biosorbent prepared from a blend of sericin and polyethylene glycol-diglycidyl ether is a viable material for removing Cu(II) ions from solutions. Biosorption depended on the pH of the solution, and the removal capacity was higher at pH values > 4. The kinetic data indicated a rapid process and fitted appropriately to the pseudo-second-order model described by the adsorption reaction. The Langmuir model satisfactorily described the equilibrium data, revealing that monolayer adsorption is the primary biosorption mechanism. Thermodynamic parameters showed exothermic biosorption, as biosorption capacity decreased with increasing temperature: 36.17 mg g^{-1} (20°C), 24.36 mg g^{-1} (40°C), and 18.76 mg g^{-1} (60°C). In addition, biosorption occurred spontaneously, and the interactions between Cu(II) ions and the biosorbent were predominantly physical. The spongy biosorbent obtained by introducing PEG-DE into sericin exhibited improved structural properties and has potential for application in fixed-bed column studies for scale-up. Finally, sericin as a novel biosorbent may reduce waste generation in the silk industry and promote residue valorization in polluted water treatment.

Acknowledgments

The authors thank the Adsorption and Ion Exchange Laboratory for performing N_2 physisorption analysis, the Electron Microscopy Center of the Federal University of Paraná for SEM for morphological analysis, and the Federal University of Paraná for making this research possible. This study was funded by the Coordenação de Aperfeiçoamento de Pessoal de Nível Superior – Brasil (CAPES) – Finance Code 001 and the Conselho Nacional de Desenvolvimento

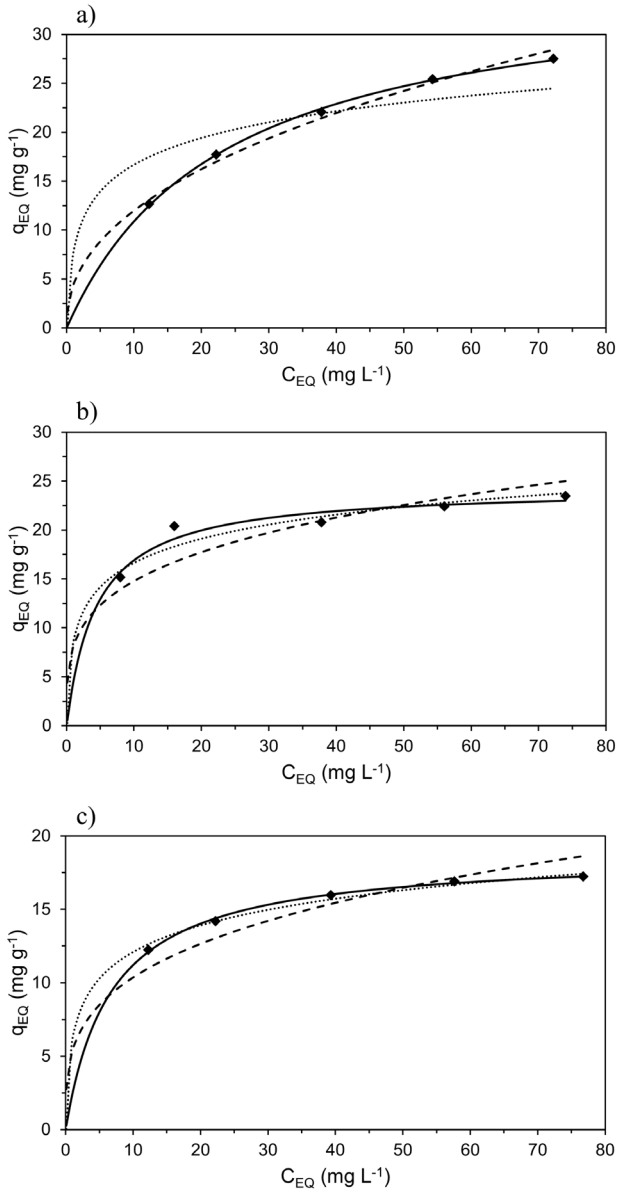

Fig. 6. Cu(II) ions biosorption equilibrium, experimental data (♦) obtained at 20°C (a), 30°C (b), and 40°C (c), and Langmuir (—), Freundlich (----), and Temkin (·····) isotherms.

Científico e Tecnológico – Brasil (CNPq) (Grant Number: 1688/2018).

References

[1] L. Joseph, B.M. Jun, J.R.V. Flora, C.M. Park, Y. Yoon, Removal of heavy metals from water sources in the developing world using low-cost materials: a review, Chemosphere, 229 (2019) 142–159.
[2] Y. Zhu, W. Fan, T. Zhou, X. Li, Removal of chelated heavy metals from aqueous solution: a review of current methods and mechanisms, Sci. Total Environ., 678 (2019) 253–266.
[3] D.G. Trikkaliotis, A.K. Christoforidis, A.C. Mitropoulos, G.Z. Kyzas, Adsorption of copper ions onto chitosan/poly(vinyl alcohol) beads functionalized with poly(ethylene glycol), Carbohydr. Polym., 234 (2020) 115890, doi: 10.1016/j.carbpol.2020.115890.
[4] M. Arbabi, N. Golshani, Removal of copper ions Cu(II) from industrial wastewater: a review of removal methods, Int. J. Epidemiol. Res., 3 (2016) 283–293.
[5] Z. Xiao, L. Zhang, L. Wu, D. Chen, Adsorptive removal of Cu(II) from aqueous solutions using a novel macroporous bead adsorbent based on poly(vinyl alcohol)/sodium alginate/$KMnO_4$ modified biochar, J. Taiwan Inst. Chem. Eng., 102 (2019) 110–117.
[6] R.V. Hemavathy, P.S. Kumar, K. Kanmani, N. Jahnavi, Adsorptive separation of Cu(II) ions from aqueous medium using thermally/chemically treated *Cassia fistula* based biochar, J. Cleaner Prod., 249 (2020) 119390, doi: 10.1016/j.jclepro.2019.119390.
[7] M. Zhang, Adsorption study of Pb(II), Cu(II) and Zn(II) from simulated acid mine drainage using dairy manure compost, Chem. Eng. J., 172 (2011) 361–368.
[8] B. Singha, S.K. Das, Adsorptive removal of Cu(II) from aqueous solution and industrial effluent using natural/agricultural wastes, Colloids Surf., B, 107 (2013) 97–106.
[9] P.V. Viotti, W.M. Moreira, O.A.A. dos Santos, R. Bergamasco, A.M.S. Vieira, M.F. Vieira, Diclofenac removal from water by adsorption on *Moringa oleifera* pods and activated carbon: mechanism, kinetic and equilibrium study, J. Cleaner Prod., 219 (2019) 809–817.
[10] T. Lopes, A. Carvalho, M. Gurgel, A. Vieira, M. Luis, M. Gurgel, Biosorption study of copper and zinc by particles produced from silk sericin–alginate blend: evaluation of blend proportion and thermal cross-linking process in particles production, J. Cleaner Prod., 137 (2016) 1470–1478.
[11] T. Anitha, P.S. Kumar, K.S. Kumar, K. Sriram, J.F. Ahmed, Biosorption of lead(II) ions onto nano-sized chitosan particle blended polyvinyl alcohol (PVA): adsorption isotherms, kinetics and equilibrium studies, Desal. Water Treat., 57 (2016) 13711–13721.
[12] G. Crini, E. Lichtfouse, L.D. Wilson, N. Morin, Conventional and non-conventional adsorbents for wastewater treatment, Environ. Chem. Lett., 17 (2019) 195–213.
[13] P. Phuengphai, T. Singjanusong, N. Kheangkhun, Removal of copper(II) from aqueous solution using chemically modified fruit peels as efficient low-cost biosorbents, Water Sci. Eng., 14 (2021) 286–294.
[14] J.M.C. Menezes, A.M. da S. Bento, F.J. de Paula Filho, J.G.M. da Costa, H.D.M. Coutinho, R.N.P. Teixeira, Kinetic and thermodynamic study of copper(II) IONS biosorption by *Caryocar Coriaceum* Wittm bark, Sustainable Chem. Pharm., 19 (2021) 100364, doi: 10.1016/j.scp.2020.100364.
[15] S. Aachhera, S. Tiwari, S. Singh, N. Nagar, H. Garg, C.S Gahan, A study on the biosorption kinetics of Cu(II) and Zn(II) ions from aqueous phase (sulphate medium) using waste sawdust generated from *Acacia nilotica* wood carpentry, Ecotoxicology, 31 (2022) 615–625.
[16] M.D. Yahya, H. Abubakar, K.S. Obayomi, Y.A. Iyaka, B. Suleiman, Simultaneous and continuous biosorption of Cr and Cu(II) ions from industrial tannery effluent using almond shell in a fixed bed column, Results Eng., 6 (2020) 100113, doi: 10.1016/j.rineng.2020.100113.
[17] J. Nastaj, M. Tuliglowicz, K. Witkiewicz, Equilibrium modeling of mono and binary sorption of Cu(II) and Zn(II) onto chitosan gel beads, Chem. Process Eng., 37 (2016) 485–501.
[18] H. Nh, K. Akli, R. Youfa, M.I. Senjawati, M. Khairati, Biosorption of Cu(II) metal ions in fixed column by using coconut husk waste, Orient. J. Chem., 34 (2018) 2192–2196.
[19] M. Gupta, H. Gupta, D.S. Kharat, Adsorption of Cu(II) by low cost adsorbents and the cost analysis, Environ. Technol. Innovation, 10 (2018) 91–101.
[20] G.G. Dusi, G.S. Marques, M.L. Kienteca, M.L. Gimenes, M.L.M.N. Cerutti, V.R. da Silva, Biosorption investigation of Cu(II) ions from aqueous solutions using sericin–alginate particles: kinetic, equilibrium, and thermodynamic, Sustainable Chem. Pharm., 25 (2022) 100601, doi: 10.1016/j.scp.2022.100601.

[21] M.L. Gimenes, V.R. Silva, F. Hamerski, M. Ribani, A.P. Scheer, Biosorption of copper(II) onto sericin powder derived from cocoons of the silkworm *Bombyx mori*: kinetics, equilibrium and thermodynamics studies, Chem. Eng. Trans., 49 (2016) 205–210.
[22] V.R. Silva, F. Hamerski, T.A. Weschenfelder, M. Ribani, M.L. Gimenes, A.P. Scheer, Equilibrium, kinetic, and thermodynamic studies on the biosorption of Bordeaux S dye by sericin powder derived from cocoons of the silkworm *Bombyx mori*, Desal. Water Treat., 57 (2016) 5119–5129.
[23] J.R. de Andrade, M.G.C. da Silva, M.L. Gimenes, M.G.A. Vieira, Bioadsorption of trivalent and hexavalent chromium from aqueous solutions by sericin-alginate particles produced from *Bombyx mori* cocoons, Environ. Sci. Pollut. Res., 25 (2018) 25967–25982.
[24] P. Vaithanomsat, V. Kitpreechavanich, Sericin separation from silk degumming wastewater, Sep. Purif. Technol., 59 (2008) 129–133.
[25] W. Tao, M. Li, R. Xie, Preparation and structure of porous silk sericin materials, Macromol. Mater. Eng., 290 (2005) 188–194.
[26] J.R. De Andrade, M.G.C. Da Silva, M.L. Gimenes, M.G.A. Vieira, Equilibrium and thermodynamic studies on adsorption of trivalent chromium by sericin-alginate particles prepared from *Bombyx mori* cocoons, Chem. Eng. Trans., 52 (2016) 169–174.
[27] K.Y. Cho, J.Y. Moon, Y.W. Lee, K.G. Lee, J.H. Yeo, H.Y. Kweon, K.H. Kim, C.S. Cho, Preparation of self-assembled silk sericin nanoparticles, Int. J. Biol. Macromol., 32 (2003) 36–42.
[28] V.R. Silva, M. Ribani, M.L. Gimenes, A.P. Scheer, High molecular weight sericin obtained by high temperature and ultrafiltration process, Procedia Eng., 42 (2012) 833–841.
[29] S. Brunauer, P.H. Emmett, E. Teller, Adsorption of gases in multimolecular layers, J. Am. Chem. Soc., 60 (1938) 309–319.
[30] B.H. Hameed, I.A.W. Tan, A.L. Ahmad, Adsorption isotherm, kinetic modeling and mechanism of 2,4,6-trichlorophenol on coconut husk-based activated carbon, Chem. Eng. J., 144 (2008) 235–244.
[31] Z. Marczenko, M. Balcerzak, Chapter 19 – Copper, Z. Marczenko, M. Balcerzak, Eds., Analytical Spectroscopy Library, Vol. 10, Elsevier, 2000, pp. 177–188. Available at: https://doi.org/10.1016/S0926-4345(00)80083-8
[32] E. Lambdin, W. V Taylor, Determination of trace copper in petroleum middle distillates with cuprizone, Anal. Chem., 40 (1968) 2196–2197.
[33] H. Qiu, L. Lv, B.C. Pan, Q.J. Zhang, W.M. Zhang, Q.X. Zhang, Critical review in adsorption kinetic models, J. Zhejiang Univ. Sci. A, 10 (2009) 716–724.
[34] A.A. Khan, R.P. Singh, Adsorption thermodynamics of carbofuran on Sn(IV) arsenosilicate in H^+, Na^+ and Ca^{2+} forms, Colloids Surf., 24 (1987) 33–42.
[35] C.J. Park, J. Ryoo, C.S. Ki, J.W. Kim, I.S. Kim, D.G. Bae, I.C. Um, Effect of molecular weight on the structure and mechanical properties of silk sericin gel, film, and sponge, Int. J. Biol. Macromol., 119 (2018) 821–832.
[36] X. Chen, K.F. Lam, S.F. Mak, K.L. Yeung, Precious metal recovery by selective adsorption using biosorbents, J. Hazard. Mater., 186 (2011) 902–910.
[37] H. Teramoto, M. Miyazawa, Molecular orientation behavior of silk sericin film as revealed by ATR infrared spectroscopy, Biomacromolecules, 6 (2005) 2049–2057.
[38] M.A. Adebayo, L.D.T. Prola, E.C. Lima, M.J. Puchana-Rosero, R. Cataluña, C. Saucier, C.S. Umpierres, J.C.P. Vaghetti, L.G. da Silva, R. Ruggiero, Adsorption of Procion Blue MX-R dye from aqueous solutions by lignin chemically modified with aluminium and manganese, J. Hazard. Mater., 268 (2014) 43–50.
[39] N.T. das G. Santos, L.F. Moraes, M.G.C. da Silva, M.G.A. Vieira, Recovery of gold through adsorption onto sericin and alginate particles chemically cross-linked by proanthocyanidins, J. Cleaner Prod., 253 (2020) 119925, doi: 10.1016/j.jclepro.2019.119925.
[40] C.H. Weng, Y.T. Lin, D.Y. Hong, Y.C. Sharma, S.C. Chen, K. Tripathi, Effective removal of copper ions from aqueous solution using base treated black tea waste, Ecol. Eng., 67 (2014) 127–133.
[41] A. Witek-Krowiak, R.G. Szafran, S. Modelski, Biosorption of heavy metals from aqueous solutions onto peanut shell as a low-cost biosorbent, Desalination, 265 (2011) 126–134.
[42] W.S.W. Ngah, S. Fatinathan, Adsorption of Cu(II) ions in aqueous solution using chitosan beads, chitosan-GLA beads and chitosan-alginate beads, Chem. Eng. J., 143 (2008) 62–72.
[43] M.N. Sahmoune, Evaluation of thermodynamic parameters for adsorption of heavy metals by green adsorbents, Environ. Chem. Lett., 17 (2019) 697–704.